J. Lundén and V. Koivunen, "Robust estimation of radar pulse modulation," in *Proceedings of the 6th IEEE International Symposium on Signal Processing and Information Technology (ISSPIT)*, Vancouver, Canada, August 27–30, 2006, pp. 271–276.

Robust Estimation of Radar Pulse Modulation

Jarmo Lundén and Visa Koivunen
Signal Processing Laboratory, SMARAD CoE
Helsinki University of Technology
P.O. Box 3000, FI-02015 TKK, Finland

Abstract — *In this paper the problem of estimating a common modulation from a group of intercepted radar pulses is addressed. A robust M-estimation technique is proposed. The M-estimation approach provides tolerance against preprocessing errors as well as to other model failures. The performance of the M-estimation technique is compared to a maximum likelihood estimation method through simulation experiments.*

Keywords — *M-estimation, radar, specific emitter identification*

I. INTRODUCTION

Automatic waveform recognition has important applications in wireless communications, spectrum management and surveillance as well as in defense applications. Among the most challenging tasks is specific emitter identification (SEI). Intrapulse information based clustering of collected radar pulses and identification of radar emitters has received increasing interest during the past few years. Time-frequency representation based approach for radar emitter identification has been proposed in [1]. In [2, 3] extracted intrapulse features are used for recognizing a specific emitter. Clustering of collected radar pulses using intrapulse information and information theoretic criteria has been studied in [4, 5].

Howard [6] has considered maximum likelihood (ML) estimation of a common modulation from a group of radar pulses followed by hypothesis testing for identifying a specific emitter. A critical stage in the estimation process is the alignment of the pulses both in time and frequency. In this paper, we propose a robust M-estimation technique for estimating a common modulation from a group of pulses. The M-estimation approach is able to downweight pulses that are misaligned in time or frequency. Such pulses would appear as outliers and consequently cause large estimation errors. It is well known that optimal ML methods are particularly sensitive to even small departures from nominal assumptions. In addition, preprocessing algorithms for aligning the pulses in time and frequency domain are proposed. In particular, a sequential cross-correlation based method for time alignment of pulses is developed.

The paper is organized as follows. Section II presents the problem and the employed signal model. Section III considers the preprocessing stage. The ML estimator is presented in Section IV, and Section V introduces the proposed M-estimators.

Simulation results are presented in Section VI. Finally, concluding remarks are given in Section VII.

II. SIGNAL MODEL

In this paper we address the problem of estimating a common modulation from a group of intercepted radar pulses. It is a crucial step in specific emitter identification. Fig. 1 illustrates the estimation process. First the intercepted radar pulses are preprocessed in order to align them in time and frequency domains. Then the common modulation profile is estimated from the aligned pulses. The symbols in Fig. 1 are defined in the following presentation of the signal model.
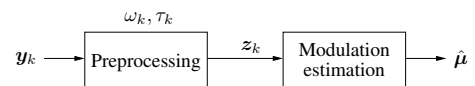
Fig. 1. Block diagram of the estimation process.

The employed discrete time signal model is presented next. Sampling rate is assumed to be high enough to record the modulations of the pulses faithfully. Furthermore, it is considered that the collection of the pulses consists of a number of fixed length vectors of N_S complex samples (i.e. one vector for each pulse) with a buffer of samples recorded before and after the pulse.

The complex pulse vectors $\boldsymbol{y}_k$, $k = 1, \ldots, N_P$, are assumed to take the form [6]

$$\boldsymbol{y}_k = A_k \boldsymbol{\mathcal{T}}(\tau_k)\boldsymbol{\Omega}(\omega_k)\boldsymbol{\mu} + \boldsymbol{\epsilon}_k, \quad k = 1, \ldots, N_P, \quad (1)$$

where A_k are the complex amplitudes of the pulses and $\boldsymbol{\mu}$ is a fixed unit vector representing the basic pulse modulation. The $\boldsymbol{\epsilon}_k$ are independent circular complex Gaussian distributed random vectors satisfying $E(\boldsymbol{\epsilon}) = \boldsymbol{0}$ and $E(\boldsymbol{\epsilon}\boldsymbol{\epsilon}^H) = \sigma^2 \boldsymbol{I}$. Here, $E(\cdot)$ denotes the expectation operator, $(\cdot)^H$ denotes the conjugate transpose, and σ^2 is the noise variance assumed to be known. $\boldsymbol{I}$ is an $N_S \times N_S$ identity matrix, where N_S is the number of samples in the pulse vectors. The parameters τ_k and ω_k are the circular time and frequency shifts required to align the kth pulse with $\boldsymbol{\mu}$.

The time and frequency shift operators $\boldsymbol{\mathcal{T}}(\tau)$ and $\boldsymbol{\Omega}(\omega)$ may

be written as follows [6]

$$\mathbf{\Omega}(\omega)_{kn} = \exp(-jn\omega)\delta_{kn}, \qquad (2)$$

$$\mathbf{T}(\tau) = \mathbf{\mathcal{F}}^{-1}\mathbf{\Omega}(2\pi\tau)\mathbf{\mathcal{F}}, \qquad (3)$$

where δ_{kn} is the Kronecker delta (i.e. $\delta_{kn} = 1$, if $k = n$, otherwise 0), j is the imaginary unit, and $\mathbf{\mathcal{F}}$ denotes the discrete Fourier transform matrix

$$\mathbf{\mathcal{F}}_{kn} = \exp(-j2\pi kn/N_S)/\sqrt{N_S}. \qquad (4)$$

The simplified model, obtained by first aligning the data in time and frequency, is given by [6]

$$\mathbf{z}_k = A_k\boldsymbol{\mu} + \boldsymbol{\epsilon}'_k, \quad k = 1,\dots,N_P, \qquad (5)$$

where

$$\mathbf{z}_k = \mathbf{\Omega}(\omega_k)^H \mathbf{T}(\tau_k)^H \mathbf{y}_k, \quad k = 1,\dots,N_P. \qquad (6)$$

The noise distribution remains the same after transformation since matrices $\mathbf{T}(\tau)$ and $\mathbf{\Omega}(\omega)$ are unitary. Thus, the joint probability density for the random vectors $\mathbf{z}_k$ is

$$f(\{\mathbf{z}\}|\{A\},\boldsymbol{\mu}) = (\pi\sigma^2)^{-N_S N_P}$$
$$\times \exp\left(-\frac{1}{\sigma^2}\sum_{k=1}^{N_P}(\mathbf{z}_k - A_k\boldsymbol{\mu})^H(\mathbf{z}_k - A_k\boldsymbol{\mu})\right). \qquad (7)$$

The employed signal model has been previously used in [6].

III. PREPROCESSING

The goal of preprocessing is to estimate the time and frequency shift parameters τ_k and ω_k needed for aligning the pulses with the basic profile $\boldsymbol{\mu}$. Furthermore, the estimates of τ_k and ω_k are assumed to be exact. Consequently, the simplified model in (5) may be employed after preprocessing.

In this section we propose novel preprocessing algorithms. The time alignment is improved by using a cross-correlation based algorithm. This can be combined with adaptive thresholding of the leading edge of the pulse [7]. For carrier frequency estimation we employ the Lank, Reed, Pollon frequency estimator [8]. It is computationally very efficient and provides an estimate of the mean frequency.

Due to the fact that the time alignment algorithm is based on cross-correlation of the pulses, the frequency alignment has to be performed prior to the time alignment.

A. Frequency Alignment

The pulses may have different carrier frequencies due to frequency agile radars as well as possibly different Doppler shifts. Consequently, carrier frequency estimation and alignment has to be performed separately for each pulse.

An estimate of the carrier frequency of the pulse $\mathbf{y}_k$ may be obtained by [8,9]

$$\hat{\omega}_{\mathbf{y}_k} = \angle \sum_{n=2}^{N_S} \mathbf{y}_k(n)\mathbf{y}_k^*(n-1), \qquad (8)$$

where $\angle$ denotes the phase angle, and $*$ denotes the complex conjugate. This estimator does not have as good performance as the ML frequency estimator [10] for single frequency estimation, see e.g. [11]. However, unlike the ML estimator the estimator in (8) provides the estimate of the mean frequency. Thus, it provides an unambiguous estimate also for signals that do not have unique maximum in their frequency spectrum. For instance, frequency shift keying (FSK) modulated signals can have such a frequency spectrum.

After carrier frequencies have been estimated, the pulses are transferred to the baseband

$$\mathbf{z}_k(n) = \mathbf{\Omega}(\hat{\omega}_{\mathbf{y}_k})^H \mathbf{y}_k, \quad k = 1,\dots,N_P. \qquad (9)$$

B. Time Alignment

In order to align the pulses in time domain, the pulses $\mathbf{z}_k$, $k = 1,\dots,N_P$, are first rank ordered into a descending order based on signal-to-noise ratio (SNR). That is, the ordering is such that the pulse $\mathbf{z}_1$ has the largest SNR while the pulse $\mathbf{z}_{N_P}$ has the smallest SNR. Then the pulses are aligned in time using the following procedure:

For $k = 2,\dots,N_P$,

1. Calculate $c_j(\tau) = |\mathbf{z}_j^H \mathbf{z}_k(\tau)|$, $\tau = 0,\dots,N_S - 1$, for all $j = 1,\dots,k-1$. Here $\mathbf{z}_k(\tau)$ denotes τ samples circularly shifted version of $\mathbf{z}_k$.

2. Time shift of the kth pulse is given by $\hat{\tau}_k = \arg\max_\tau \sum_{j=1}^{k-1} c_j(\tau)$.

3. Shift the kth pulse circularly by $\hat{\tau}_k$ samples, i.e. $\mathbf{z}_k = \mathbf{z}_k(\hat{\tau}_k)$.

In order to reduce the computational complexity of the time alignment, adaptive thresholding of the leading edge of the pulse [7] may be used to provide an initial estimate. Then the cross-correlations of the pulses can be calculated only for the small time shifts (i.e. a few samples left or right) from the initial coarse estimate obtained by adaptive thresholding.

IV. MAXIMUM LIKELIHOOD (ML) ESTIMATOR

The proposed M-estimation method is a generalization of ML estimator. Hence, conventional ML estimator is presented first. The likelihood function (7) is maximized with respect to A_k by choosing [6]

$$\hat{A}_k = \boldsymbol{\mu}^H \mathbf{z}_k, \quad k = 1,\dots,N_P, \qquad (10)$$

272

where the simplified model has been used. A reduced likelihood function is obtained by substituting the $\hat{A}_k$ to the likelihood function. Optimization of the reduced likelihood function may be performed iteratively by using the *power method* [6]

$$\hat{\boldsymbol{\mu}}_{j+1} = \frac{\sum_{k=1}^{N_P}(\boldsymbol{z}_k^H \hat{\boldsymbol{\mu}}_j)\boldsymbol{z}_k}{\left\|\sum_{k=1}^{N_P}(\boldsymbol{z}_k^H \hat{\boldsymbol{\mu}}_j)\boldsymbol{z}_k\right\|}. \tag{11}$$

Initial estimate to ML estimate of $\boldsymbol{\mu}$, can be chosen as $\hat{\boldsymbol{\mu}}_0 = \boldsymbol{z}_{\max}/\|\boldsymbol{z}_{\max}\|$ where $\boldsymbol{z}_{\max}$ is the pulse having largest SNR [6]. The simulation results in [6] indicate that the first iteration estimate $\hat{\boldsymbol{\mu}}_1$ has equal statistical performance as the full ML estimator.

V. ROBUST ESTIMATION ALGORITHM

The time and frequency alignment process is critical to the estimation performance. A failure in preprocessing can result in misaligned pulses, and consequently outliers. In addition, pulses suffering from multipath and interference from other emitters as well as incorrectly clustered pulses coming from different emitters can be considered as outliers. The ML estimator is known to be highly sensitive to outliers. In fact, in case Gaussian noise model is used their influence on parameter estimates is unbounded. Hence, robust estimators that have close to optimal performance at nominal conditions and work reliably at the presence of outliers are of interest. Robust M-estimators reduce the influence of the outliers by minimizing an objective function defined as

$$J = \sum_i \rho(r_i/s_i), \tag{12}$$

where r_i is the residual error of the ith observation, i.e. the difference between the ith observation and its estimated value, and s_i is its corresponding scale. The ρ function is a symmetric real-valued function that reduces the influence of the outliers. The Huber ρ function used in this work is given by [12]

$$\rho(r) = \begin{cases} r^2/2, & \text{for } |r| < k \\ k|r| - k^2/2, & \text{for } |r| \geq k, \end{cases} \tag{13}$$

where k is a tuning constant. The derivative of $\rho(r)$ is the ψ function. The Huber ψ function that makes the influence of outliers bounded is given by

$$\psi(r) = \begin{cases} r, & \text{for } |r| < k \\ k\,\text{sign}(r), & \text{for } |r| \geq k. \end{cases} \tag{14}$$

The M-estimate may be found, for example, by using an iterative reweighted least-squares (IRLS) procedure. For the radar pulse modulation the procedure is given as follows

1. Initialize the weights $w_{kn} = 1$, $k = 1, \ldots, N_P$, $n = 1, \ldots, N_S$, and set $i = 0$.
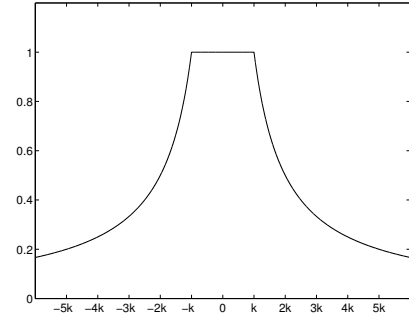
Fig. 2. Huber weight function.

2. Initialize $\boldsymbol{\mu}^{(0)} = \boldsymbol{z}_{\max}/\|\boldsymbol{z}_{\max}\|$ where $\boldsymbol{z}_{\max}$ is the pulse having the largest SNR.

3. Solve the following weighted least-squares problem

$$\min \sum_{k=1}^{N_P} \sum_{n=1}^{N_S} w_{kn}|\boldsymbol{z}_k(n) - A_k\boldsymbol{\mu}(n)|^2, \tag{15}$$

in order to get $\boldsymbol{\mu}^{(i+1)}$ and $A_k^{(i+1)}$, $k = 1, \ldots, N_P$.

4. Recalculate the weights

$$w_{kn} = w\left(\frac{|\boldsymbol{z}_k(n) - A_k^{(i+1)}\boldsymbol{\mu}^{(i+1)}(n)|}{\sigma}\right).$$

5. If the change in the error is small, stop. That is, stop if

$$\frac{L^{(i)}}{L^{(i+1)}} < 1 + \beta,$$

where $L^{(i)} = \sum_{k=1}^{N_P}\sum_{n=1}^{N_S}|\boldsymbol{z}_k(n) - A_k^{(i)}\boldsymbol{\mu}^{(i)}(n)|^2$ and β is a small number, such as 0.001. Otherwise increment i and go back to 3.

The weight function $w(r)$ is defined as $\psi(r)/r$. Thus, the Huber weight function used in this work is given by

$$w(r) = \begin{cases} 1, & \text{for } |r| < k \\ k/|r|, & \text{for } |r| \geq k. \end{cases} \tag{16}$$

Fig. 2 depicts the Huber weight function. Value $k = 1.345$ was employed in the simulations. Note that the residual errors are normalized wrt. scale $s_i = \sigma$, i.e. the standard deviation of the noise which is assumed to be known. If σ is not known a simple and robust estimate of the scale s_i is the median of the absolute deviations from the median (MAD) [13].

In step 3 of the above IRLS procedure, a weighted least-squares problem needs to be solved. In the following, iterative methods for solving the problem for two different weighting approaches are presented. In the first approach, each pulse has a distinct weight but all the samples from the same pulse have

273

equal weight. This enables downweighting of the pulses that cause large errors, for instance, due to misalignment. However, at same time it means that even a single outlying sample within a pulse can cause the algorithm unnecessarily downweight the whole pulse. In the second approach each sample has a separate weight. That is, it enables different weights for different parts of individual pulses. This should be more suitable, for example, when the noise has impulsive components. However, it is computationally more expensive than the first weighting approach.

A. M-estimator Using Equal Weights within Pulses

Under Gaussian noise assumption, ML estimation corresponds to minimizing the sum of squared errors, see [6]. Starting from the weighted least-squares problem

$$L = \sum_{k=1}^{N_P} w_k (z_k - A_k \boldsymbol{\mu})^H (z_k - A_k \boldsymbol{\mu}), \qquad (17)$$

where w_k, $k = 1, \ldots, N_P$, are scalar weights for the pulses.

We may rewrite (17) as follows

$$L = \sum_{k=1}^{N_P} w_k (z_k^H z_k - |\boldsymbol{\mu}^H z_k|^2) + \sum_{k=1}^{N_P} w_k |A_k - \boldsymbol{\mu}^H z_k|^2, \ (18)$$

and minimize it with respect to A_k by choosing

$$\hat{A}_k = \boldsymbol{\mu}^H z_k, \quad k = 1, \ldots, N_P. \qquad (19)$$

By substituting $\hat{A}_k$ from (19) for A_k in (18), a reduced cost function is obtained

$$L' = \sum_{k=1}^{N_P} w_k (z_k^H z_k - |\boldsymbol{\mu}^H z_k|^2). \qquad (20)$$

Minimizing (20) with respect to $\boldsymbol{\mu}$ is equivalent to the following maximization task

$$\arg \max_{\boldsymbol{\mu}} \sum_{k=1}^{N_P} w_k |\boldsymbol{\mu}^H z_k|^2 = \arg \max_{\boldsymbol{\mu}} \boldsymbol{\mu}^H (\sum_{k=1}^{N_P} w_k z_k z_k^H) \boldsymbol{\mu}$$
$$= \arg \max_{\boldsymbol{\mu}} \boldsymbol{\mu}^H \boldsymbol{Z}_w \boldsymbol{\mu}. \qquad (21)$$

This quadratic expression is maximized if $\boldsymbol{\mu}$ is equal to the eigenvector of $\boldsymbol{Z}_w$ corresponding to the largest eigenvalue [14, p. 176]. The *power method* is employed to find the eigenvector, i.e.

$$\hat{\boldsymbol{\mu}}_{j+1} = \boldsymbol{Z}_w \hat{\boldsymbol{\mu}}_j = \sum_{k=1}^{N_P} w_k (z_k^H \hat{\boldsymbol{\mu}}_j) z_k, \qquad (22)$$

$$\hat{\boldsymbol{\mu}}_{j+1} = \hat{\boldsymbol{\mu}}_{j+1} / ||\hat{\boldsymbol{\mu}}_{j+1}||. \qquad (23)$$

Note that the update of the weights w_k in the IRLS procedure is in this case given by

$$w_k = w \left(\frac{||z_k - \hat{A}_k \hat{\boldsymbol{\mu}}||}{\sigma \sqrt{N_S}} \right).$$

B. M-estimator Using Different Weights within Pulses

Using separate weight for each sample, the weighted least-squares problem can be written as

$$L = \sum_{k=1}^{N_P} (z_k - A_k \boldsymbol{\mu})^H \boldsymbol{W}_k (z_k - A_k \boldsymbol{\mu}), \qquad (24)$$

where the $\boldsymbol{W}_k$ are diagonal matrices containing the weights for the samples. In order to minimize (24), it is differentiated with respect to A_k^* and $\boldsymbol{\mu}^*$ and the derivatives are set to zero

$$\frac{\partial L}{\partial A_k^*} = -\boldsymbol{\mu}^H \boldsymbol{W}_k z_k + A_k \boldsymbol{\mu}^H \boldsymbol{W}_k \boldsymbol{\mu} = 0, \ k = 1, \ldots, N_P, \qquad (25)$$

$$\frac{\partial L}{\partial \boldsymbol{\mu}^*} = \sum_{k=1}^{N_P} (-A_k^* \boldsymbol{W}_k z_k + |A_k|^2 \boldsymbol{W}_k \boldsymbol{\mu}) = \boldsymbol{0}. \qquad (26)$$

Solving (25) and (26), gives

$$\hat{A}_k = \frac{1}{\boldsymbol{\mu}^H \boldsymbol{W}_k \boldsymbol{\mu}} \boldsymbol{\mu}^H \boldsymbol{W}_k z_k, \quad k = 1, \ldots, N_P, \qquad (27)$$

$$\hat{\boldsymbol{\mu}} = \left(\sum_{k=1}^{N_P} |A_k|^2 \boldsymbol{W}_k \right)^{-1} \sum_{k=1}^{N_P} A_k^* \boldsymbol{W}_k z_k. \qquad (28)$$

Note that the matrix inverse in (28) is easy to compute since the matrices $\boldsymbol{W}_k$ are diagonal.

In order to find an estimate of $\boldsymbol{\mu}$, the following steps are repeated until convergence

$$(\hat{A}_k)_{j+1} = \frac{1}{\hat{\boldsymbol{\mu}}_j^H \boldsymbol{W}_k \hat{\boldsymbol{\mu}}_j} \hat{\boldsymbol{\mu}}_j^H \boldsymbol{W}_k z_k, \quad k = 1, \ldots, N_P, \quad (29)$$

$$\hat{\boldsymbol{\mu}}_{j+1} = \left(\sum_{k=1}^{N_P} |(\hat{A}_k)_{j+1}|^2 \boldsymbol{W}_k \right)^{-1} \sum_{k=1}^{N_P} (\hat{A}_k^*)_{j+1} \boldsymbol{W}_k z_k,$$
$$\qquad (30)$$

$$\hat{\boldsymbol{\mu}}_{j+1} = \hat{\boldsymbol{\mu}}_{j+1} / ||\hat{\boldsymbol{\mu}}_{j+1}||. \qquad (31)$$

Choosing the initial estimate in IRLS is important. If conventional least-squares (ML in Gaussian noise) is used, the optimization may get stuck in a local minimum when using separate weights for each sample. Hence, it is beneficial to recalculate the weights in the IRLS algorithm at step $i = 0$ before solving the least-squares problem in step 3.

VI. SIMULATION RESULTS

In this section the performance of the ML and M-estimators is compared using two test pulses. Fig. 3 plots the complex test signals. The first test signal is a linear frequency modulated (LFM) pulse and the second is a Costas 4 coded pulse, i.e. a FSK pulse with 4 different frequencies.

In the first simulation, the performance of the ML and M-estimators is studied as a function of the SNR. Figs. 4 and 5

274

(a) LFM   (b) Costas 4
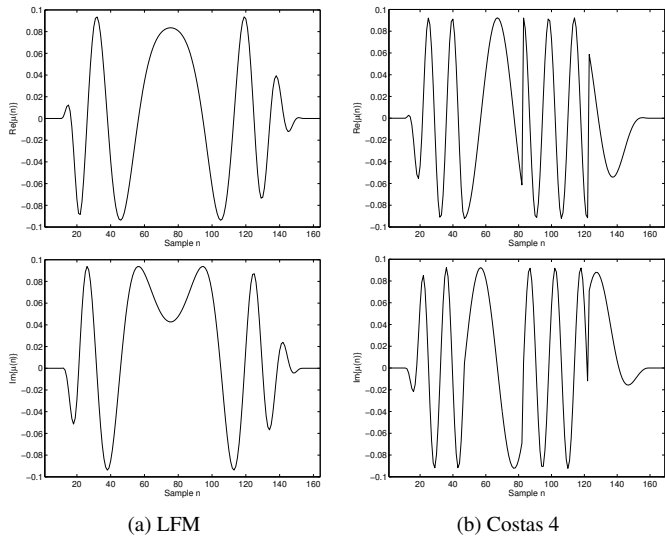
Fig. 3. Real and imaginary parts of the test signals.
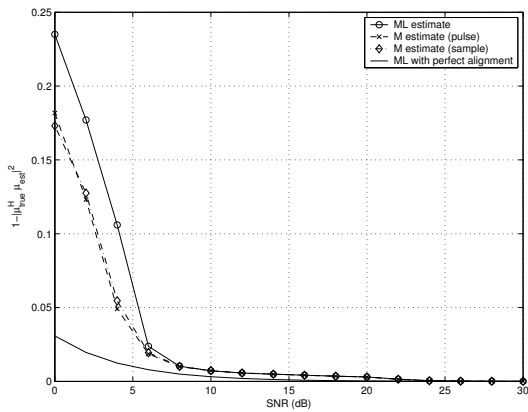
Fig. 4. $\left(1 - |\boldsymbol{\mu}_{\text{true}}^H \hat{\boldsymbol{\mu}}|^2\right)$ vs. SNR for the ML and M-estimators for 30 LFM pulses. The M-estimators have better performance at low SNR regime due to misalignment of the pulses.

show $\left(1 - |\boldsymbol{\mu}_{\text{true}}^H \hat{\boldsymbol{\mu}}|^2\right)$ versus SNR for 30 LFM and Costas pulses, respectively. The curves are averages over 500 Monte Carlo experiments. Note that also the ML estimator uses the preprocessing algorithms proposed in this paper in all simulations. The ML estimator performance with perfectly aligned pulses is plotted as well. This curve provides a lower bound for the performance of other estimators.

It can be seen that the M-estimators have better performance than the ML estimator at low SNR regime. This is due to the fact that the M-estimators downweight the pulses that are misaligned after preprocessing. Consequently, their influence on the final estimate is reduced.

In the second experiment, the performance of the estimators was studied as a function of the number of pulses used to calculate the estimate. This experiment was conducted using the LFM pulse for two different SNR regimes. Fig. 6 depicts the estimation performances when the pulse SNRs are between 3
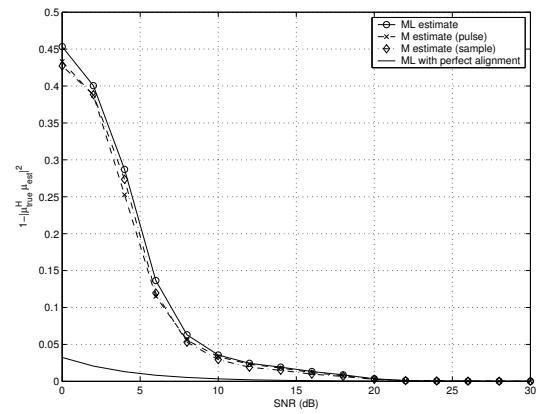
Fig. 5. $\left(1 - |\boldsymbol{\mu}_{\text{true}}^H \hat{\boldsymbol{\mu}}|^2\right)$ vs. SNR for the ML and M-estimators for 30 Costas 4 pulses. The M-estimators have better performance at low and moderate SNR regime due to misalignment of the pulses.
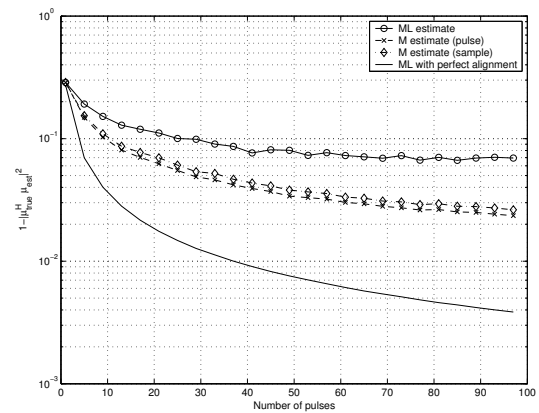
Fig. 6. $\left(1 - |\boldsymbol{\mu}_{\text{true}}^H \hat{\boldsymbol{\mu}}|^2\right)$ vs. number of pulses for the ML and M-estimators for LFM pulses with SNRs between 3 and 5 dB. The M-estimators have better performance at low SNR regime due to misalignment of the pulses.

and 5 dB. The curves are averages over 1000 Monte Carlo experiments. Again, the M-estimators have better performance than the ML estimator due to downweighting of the misaligned pulses. The estimation performance might not yet allow identification of the specific emitter. However, it should improve the probability of correctly classifying the emitter type. Fig. 7 illustrates the performance at a higher SNR regime between 18 and 30 dB where specific emitter identification should be possible. It can be seen that the ML and M-estimators have almost comparable performance. The ML-estimator is slightly better than, especially, the M-estimator using sample weights. The gap between estimator performance curves and the curve obtained with perfect alignment indicates that there is probably a small frequency offset in the final estimate.

Gaussian noise assumption may not always hold in practical applications. In the final experiment, the noise distribution is a mixture of two complex Gaussian distributions with different variances, i.e. the noise distribution is $0.95 N_C(0, \sigma^2) + 0.05 N_C(0, 25\sigma^2)$. The purpose of the second term is to model

275
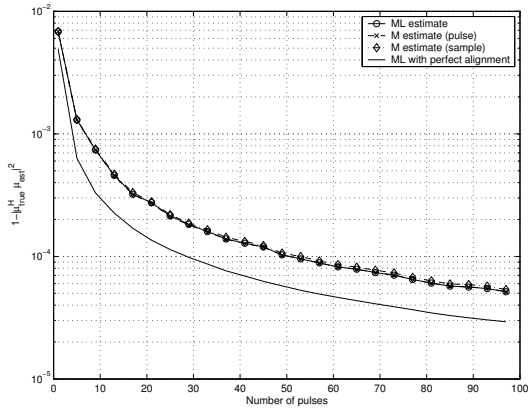
Fig. 7. $(1 - |\boldsymbol{\mu}_{\text{true}}^{H}\hat{\boldsymbol{\mu}}|^2)$ vs. number of pulses for the ML and M-estimators for LFM pulses with SNRs between 18 and 30 dB. The estimators have almost comparable performance. The M-estimator with sample weights has slightly worse performance.
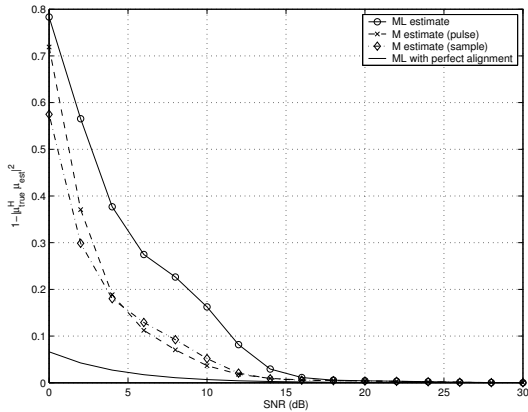
Fig. 8. $(1 - |\boldsymbol{\mu}_{\text{true}}^{H}\hat{\boldsymbol{\mu}}|^2)$ vs. SNR for the ML and M-estimators for 30 LFM pulses in non-Gaussian noise with a density of $0.95 N_C(0, \sigma^2) + 0.05 N_C(0, 25\sigma^2)$. SNR is measured compared to noise power σ^2. The M-estimators outperform the ML estimator in non-Gaussian noise.

the outliers caused by interference. Fig. 8 depicts the performance of the estimators for 30 LFM pulses in non-Gaussian noise as a function of the SNR. The SNR is measured compared to σ^2. The figure shows that the M-estimators have clearly better performance in non-Gaussian noise situation than the ML estimator.

VII. CONCLUSION

In this paper a robust M-estimator of a common modulation from a group of radar pulses was proposed. In addition, a new time alignment algorithm based on cross-correlation was proposed for aligning the intercepted pulses in time domain.

The simulation experiments showed that the M-estimators provide better tolerance against preprocessing errors than the ML estimator. This facilitates specific emitter identification at lower SNR regime and improves the probability of classifying

the emitter type correctly at given SNR. In addition, the M-estimators perform well also in non-standard noise conditions such as non-Gaussian noise. However, to further improve the estimation performance more work is needed for better alignment of the pulses in both time and frequency.

REFERENCES

[1] B. W. Gillespie and L. E. Atlas, "Optimization of time and frequency resolution for radar transmitter identification," in *Proc. IEEE Int'l Conference on Acoustics, Speech, and Signal Processing 1999 (ICASSP '99)*, vol. 3, Phoenix, AZ, USA, Mar. 15–19, 1999, pp. 1341–1344.

[2] A. Kawalec and R. Owczarek, "Radar emitter recognition using intra-pulse data," in *Proc. 15th Int'l Conference on Microwaves, Radar and Wireless Communications (MIKON 2004)*, vol. 2, May 17–19, 2004, pp. 435–438.

[3] A. Kawalec and R. Owczarek, "Specific emitter identification using intrapulse data," *European Radar Conference 2004*, Amsterdam, Oct. 2004, pp. 249–252.

[4] J. Liu, S. Gao, Z.-Q. Luo, T. N. Davidson, and J. P. Y. Lee, "The minimum description length criterion applied to emitter number detection and pulse classification," in *Proc. 9th IEEE Signal Processing Workshop on Statistical Signal and Array Processing 1998*, Portland, OR, USA, Sep. 14–16, 1998, pp. 172–175.

[5] Y. Zhou, and J. P. Y. Lee, "Combining clustering techniques and information theoretic criteria based approach for emitter number detection in ESM applications," in *Proc. of the Thirty-Third Asilomar Conference on Signals, Systems, and Computers*, vol. 1, Pacific Grove, CA, USA, Oct. 24–27, 1999, pp. 474–478.

[6] S. D. Howard, "Estimation and correlation of radar pulse modulations for electronic support," in *Proc. IEEE Aerospace Conference 2003*, vol. 5, Mar. 8–15, 2003, pp. 2065–2072.

[7] D. J. Torrieri, "Statistical theory of passive location systems," *IEEE Trans. Aerosp. Electron. Syst.*, vol. 20, pp. 183-198, Mar. 1984.

[8] G. W. Lank, I. S. Reed, and G. E. Pollon, "A semicoherent detection and Doppler estimation statistic," *IEEE Trans. Aerosp. Electron. Syst.*, vol. AES-9, pp. 151–165, Mar. 1973.

[9] S. Kay, "A fast and accurate single frequency estimator," *IEEE Trans. Acoust., Speech, Signal Processing*, vol. 37, no. 12, pp. 1987–1990, Dec. 1989.

[10] D. C. Rife and R. R. Boorstyn, "Single-tone parameter estimation from discrete-time observations," *IEEE Trans. Inform. Theory*, vol. IT-20, no. 5, pp. 591–598, Sep. 1974.

[11] V. Clarkson, "Efficient single frequency estimators," in *Proc. Int'l Sympos. Signal Processing Appl.*, Aug. 1992, pp. 327–330.

[12] P. J. Huber, *Robust statistics*, John Wiley & Sons, New York, 1981.

[13] F. R. Hampel, "The influence curve and its role in robust estimation," *J. Am. Statist. Assoc.*, vol. 69, no. 346, pp. 383–393, Jun. 1974.

[14] R. A. Horn and C. R. Johnson, *Matrix analysis*, Cambridge, 1985.